Tellus SERIES B CHEMICAL AND PHYSICAL METEOROLOGY
PUBLISHED BY THE INTERNATIONAL METEOROLOGICAL INSTITUTE IN STOCKHOLM

Tellus (2011), 63B, 875–890
Printed in Singapore. All rights reserved

Near-global aerosol mapping in the upper troposphere and lowermost stratosphere with data from the CARIBIC project

By JOST HEINTZENBERG[1]*, MARKUS HERMANN[1], ANDREAS WEIGELT[1], ANTONY CLARKE[2], VLADIMIR KAPUSTIN[2], BRUCE ANDERSON[3], KENNETH THORNHILL[3], PETER VAN VELTHOVEN[4], ANDREAS ZAHN[5] and CARL BRENNINKMEIJER[6], [1]*Leibniz Institute for Tropospheric Research, Permoserstr. 15, 04318 Leipzig, Germany;* [2]*University of Hawaii, Department of Oceanography, Honolulu, HI 96822, USA;* [3]*NASA Langley Research Center, Hampton, VA 23681, USA;* [4]*Royal Netherlands Meteorological Institute (KNMI), 3730 AE de Bilt, Netherlands;* [5]*Institute for Meteorology and Climate Research, Karlsruhe Institute of Technology (KIT), 76021 Karlsruhe, Germany;* [6]*Max Planck Institute for Chemistry, Atmospheric Chemistry Division, 6500 Mainz, Germany*

(Manuscript received 11 October 2010; in final form 22 June 2011)

ABSTRACT

This study extrapolates aerosol data of the CARIBIC project from 1997 until June 2008 in along trajectories to compose large-scale maps and vertical profiles of submicrometre particle concentrations in the upper troposphere and lowermost stratosphere (UT/LMS). The extrapolation was validated by comparing extrapolated values with CARIBIC data measured near the respective trajectory position and by comparing extrapolated CARIBIC data to measurements by other experiments near the respective trajectory positions. Best agreement between extrapolated and measured data is achieved with particle lifetimes longer than the maximum length of used trajectories. The derived maps reveal regions of strong and frequent new particle formation, namely the Tropical Central and Western Africa with the adjacent Atlantic, South America, the Caribbean and Southeast Asia. These regions of particle formation coincide with those of frequent deep convective clouds. Vertical particle concentration profiles for the troposphere and the stratosphere confirm statistically previous results indicating frequent new particle formation in the tropopause region. There was no statistically significant increase in Aitken mode particle concentration between the first period of CARIBIC operation, 1997–2002, and the second period, 2004–2009. However, a significant increase in concentration occurred within the latter period when considering it in isolation.

1. Introduction

Since 1997, a unique combination of in situ gas and aerosol particle sensors plus air and particle samplers has been deployed on a regular basis successively on two different commercial long-range aircraft in the CARIBIC project (Brenninkmeijer et al., 1999; Brenninkmeijer et al., 2007). The aerosol-related results of the CARIBIC project have generated a host of publications elucidating particle characteristics and origin along the CARIBIC flight tracks (cf. the CARIBIC website www.caribic-atmospheric.com/). To date, these publications built exclusively on aerosol data as measured along the CARIBIC aircraft flight routes. However, the upper troposphere and lowermost stratosphere (UT/LMS) region exhibits characteristics that would justify extrapolating the measured data to a much wider geographical region than covered by the flight tracks alone: Persistent high wind speeds, large distance to particle sources near the Earth's surface and (compared to the lower atmosphere) smaller risks of cloud scavenging of aerosol particles and of their precursors. Consequently, this study connects systematically air mass backward and forward trajectories calculated for locations along the CARIBIC flight tracks with particle number concentrations measured in different size ranges. This approach is not new and was, for instance, used to extend the ozone measurements of the Measurements of OZone, water vapour, carbon monoxide and nitrogen oxides by in-service AIrbus airCraft (MOZAIC) project by Stohl et al. (2001). However, because of the sparseness of aerosol measurements in the free troposphere or above, it

*Corresponding author.
e-mail: jost@tropos.de
DOI: 10.1111/j.1600-0889.2011.00578.x

was not applied to aerosol particles in this region up to now. By using the complete CARIBIC aerosol data set from 1997 to June 2008 global aerosol maps were constructed and are presented in this paper. The large data set is also analysed for information on the vertical and seasonal distribution of particle concentrations.

Extrapolating our aerosol data along trajectories also allowed both, a self-validation of the results and a validation with independent external aerosol data that were measured far away from the CARIBIC flight routes (www.caribic-atmospheric.com/). From these validation exercises, finally, we draw conclusions about the possible lifetimes of submicrometre particles in the UT/LMS.

2. Database

The used database of CARIBIC flights starts on 25 November 1997 and ends on 19 June 2008. In this period, there was a break for airline changeover from LTU International Airways to Deutsche Lufthansa (LH) from May 2002 to December 2004. The two parts of the data set are approximately of equal size, 44% of the measurements are from LTU flights and 56% from LH flights. The whole data set comprises a total of 148 intercontinental flights (Fig. 1, top panel). About 77% of the measurements fall into the latitude band between 20° and 55°N. The majority of measurements were carried out at cruise altitudes between

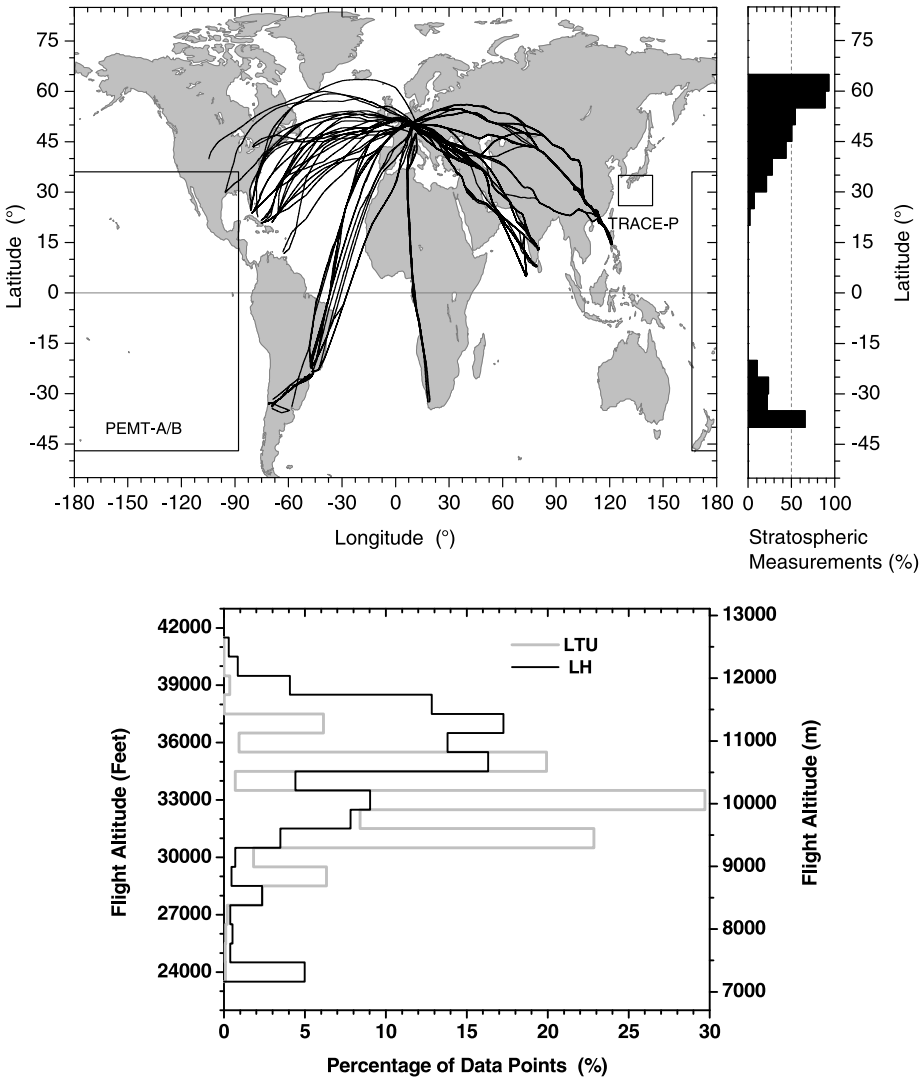

Fig. 1. Top panel: Flight tracks of all CARIBIC flights included in this study, covering the time period 25 November 1997 to 19 June 2008. The two regions, in which extrapolated CARIBIC data were compared to research aircraft measurements, are marked as boxes. The fraction of stratospheric measurements per 5° latitude bin is given in the right graph. Bottom panel: Histograms of the CARIBIC measurement altitudes for the two periods 1997–2002 (LTU, grey) and 2004–2008 (LH, black). Bins at 24.000 and 41.000 feet include all measurements below or above this altitude, respectively.

8 and 12 km (Fig. 1, bottom panel), with a latitude-dependent fraction of stratospheric measurements (Fig. 1, top panel).

In CARIBIC, particle number concentrations in three particle size ranges (N_4: $\geq$ 4 nm, N_{12}: $\geq$ 12 nm and N_{18}: $\geq$ 18 nm diameter) are measured with 2 s time resolution by condensation particle counters (CPCs). The difference of the first two channels yields the number concentration of nucleation mode particles, N_{4-12}. Although nominally the sum of Aitken plus accumulation mode particles, for most cases N_{12} can be considered the number concentration of Aitken mode particles alone, as the Aitken mode generally dominates the accumulation mode in the UT (e.g. Clarke and Kapustin, 2002; Heintzenberg et al., 2002). All particle concentrations are expressed in standard temperature and pressure conditions (STP, 273.15 K, 1013.25 hPa). Details of the CPC measurements and their calibrations can be found in Hermann et al. (2001, 2003, 2005, 2007) and Hermann and Wiedensohler (2001).

As the CARIBIC aircraft is employed on a regular flight schedule, the local measurement time in a geographic region might be concentrated around specific local times of the day. There are regions with only nighttime measurements and only daytime measurements. This is particularly important for the short-lived nucleation mode particles, because of photochemistry represents being an important step in particle formation (e.g. Hermann et al., 2003). For larger particles, the influence is expected to be smaller. To indicate which regions of the CARIBIC measurements are subject to this bias, in Fig. 2, the relative fraction of daytime (06:00–18:00 local time) measurements on a 15° × 15° geocell grid is displayed. In this map, only geocells with at least 9 h of total measurement time were considered (representing 94% of the data). For the northern midlatitudes and subtropics, daytime and nighttime measurements are reasonably well balanced, as the green colours dominate (30–70% daytime measurements). However, over the Arabian Sea and South Africa, daytime measurements strongly dominate, whereas over the South America route night measurements dominate. This bias must be considered when interpreting and using the nucleation mode particle concentrations in the respective regions.

Two times per year, when switching from summer to winter flight schedule and back, there can be larger changes in the flight routes of the CARIBIC aircraft. This can cause a seasonal bias in the data. For the four major flight routes of the present data set, to India, the Caribbean, South America and Southeast Asia (93% of the flights), the summer flights amount to 60, 64, 40 and 53% of the flights on the respective routes. For the LTU, LH and all flights taken together the respective numbers are 56, 59 and 57%. Consequently, there is a small but acceptable seasonal bias towards boreal summer measurements in both parts of the data set.

The aerosol data were complemented with 48-h forward and backward trajectories calculated with the TRAJKS trajectory model at the Koninklijk Nederlands Meteorologisch Instituut (KNMI), de Bilt, Netherlands (www.knmi.nl/samenw/campaign_support/CARIBIC). This trajectory model uses wind fields from the European Centre for Medium-Range Weather Forecasts (ECMWF) hybrid sigma-pressure model. Endpoints of the backward trajectories and start points of the forward trajectories were the coordinates, every 3 min, along the CARIBIC flight tracks. Figure 3 illustrates a typical flight track with selected trajectories (both backward and forward) exemplifying the extent to which the measured data might be extrapolated on this basis.

According to the method developed in Weigelt et al. (2009), the CARIBIC trajectories were overlaid with satellite images of cloud data from the International Satellite Cloud Climatology Project (ISCCP; http://isccp.giss.nasa.gov; Rossow and Schiffer, 1991). For this analysis, the spatially and temporally high-resolved ISCCP-DX product was used. Due to the different temporal resolution of the trajectories (1 h) and the

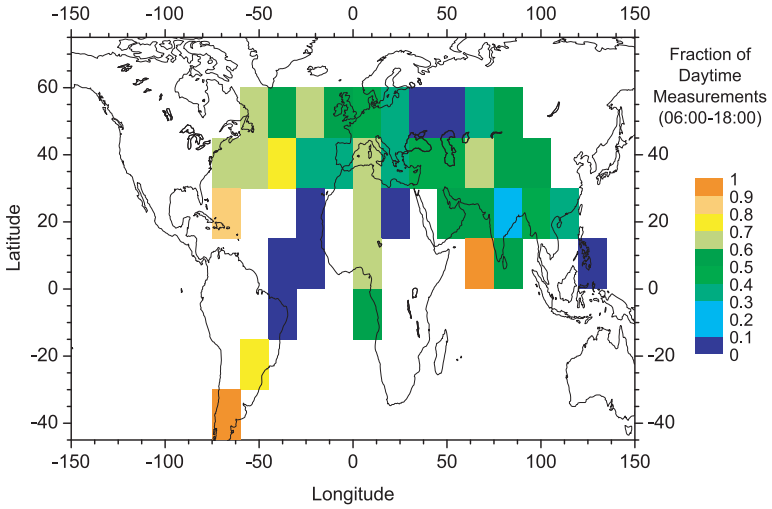

Fig. 2. Relative fraction of daytime (06:00–18:00 local time) measurements within each 15° × 15° geocell with at least 9 h of measurement time.

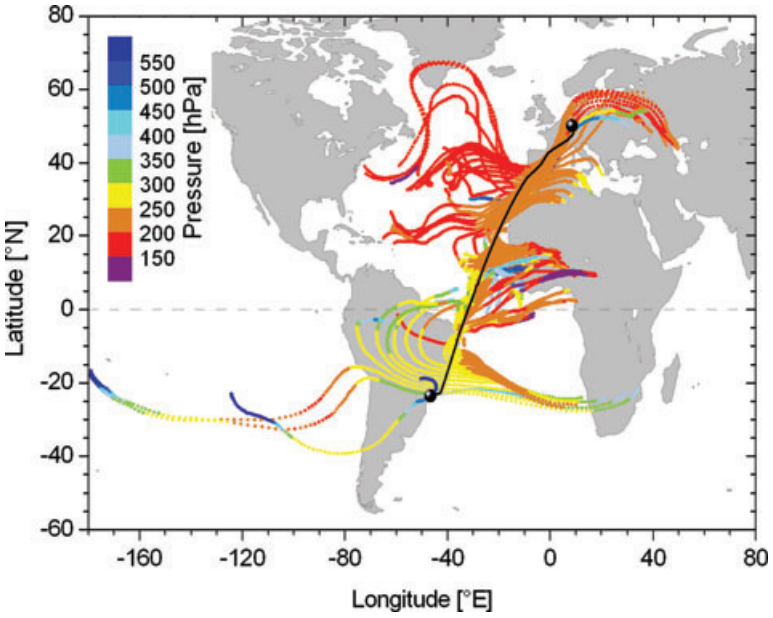

Fig. 3. Flight track and selected 48-h forward and backward trajectories of CARIBIC flight LH121 between Sao Paulo, Brazil and Frankfurt, Germany on 28 July 2005.

satellite images (3 h), the analysis algorithm contains a linear interpolation between two satellite pictures, as well as a wind-direction-dependent pixel search for the closest satellite pixel to a trajectory. To account for the uncertainties associated with long-duration trajectories (Scheele et al., 1996) and trajectories in clouds, this study analyses trajectories only in the first 48 h before or after the measurement and within this 2-d period only until a cloud contact had occurred.

To combine the cloud-analysed forward and backward trajectories with the CARIBIC data, particle number concentrations C in each size range were averaged over each ±90 s around the end and start point t_0 of each trajectory, respectively. These average values $C(t_0)$ were extrapolated backward and forward in time along the trajectories until a cloud contact occurred or the trajectory ended 2 d from the measurement, whichever occurred first. For the extrapolation, we applied the concept of size- and height-dependent aerosol residence or lifetimes in the atmosphere as developed by Jaenicke (1978, 1988), ranging from about 1 h for particles around 1 nm to several weeks for particles at the upper size limit of the aerosol intake. To account for the aging of the aerosol along the trajectory, an exponential aging function was implemented in the extrapolation algorithm for each of the three particle size ranges. The concentration $C(t)$ at a certain trajectory node at time t is thus given by

$$C(t) = C(t_0) \cdot \mathrm{e}^{-t/\tau}, \quad (1)$$

where τ is a residence time for each of the three particles size ranges. If τ is set to infinite, no aging is applied and the concentration remains constant along the trajectory. The chosen form of the aging function is based on the assumptions that clouds are the major sources and sinks for UT/LMS submicrometre particles (Weigelt et al., 2009) and that in absence of cloud contacts particle number concentrations decrease because of coagulation processes. This approach neglects of course other source processes like particle formation in the first 24 h after cloud contact (which certainly may take place) or aircraft emissions, of which the latter, however, should be small, compared to the direct cloud source (Hermann et al., 2008). As the used extrapolation algorithm is based on strong simplifications of aerosol dynamics and hence bears large uncertainties, we validated our approach with two methods as described in Section 3.

The availability of current ISCCP data constrained our total data set to the time before the end of June 2008. Nevertheless, all together about 1.5 million extrapolated data points were available for the statistical analysis. As the extrapolated values are obtained every hour along the forward and backward trajectories, about 98% of the total data used to generate the following profiles and maps are extrapolated. Again, the validation methods are used to discuss how representative the results are.

3. Validation of extrapolation method

The number of statistically firm in situ aerosol data sets in the UT/LMS is small, limiting the possibilities of validating our measurements and trajectory-extrapolations. In the following section, we approached the validation problem from two sides.

3.1. Internal validation

Our method of extrapolating the measured number concentrations along forward and backward trajectories allowed for a self-validation of the extrapolation. We compare the statistics of aerosol concentration directly measured by the CARIBIC aircraft in a specific geocell with values determined by mapping

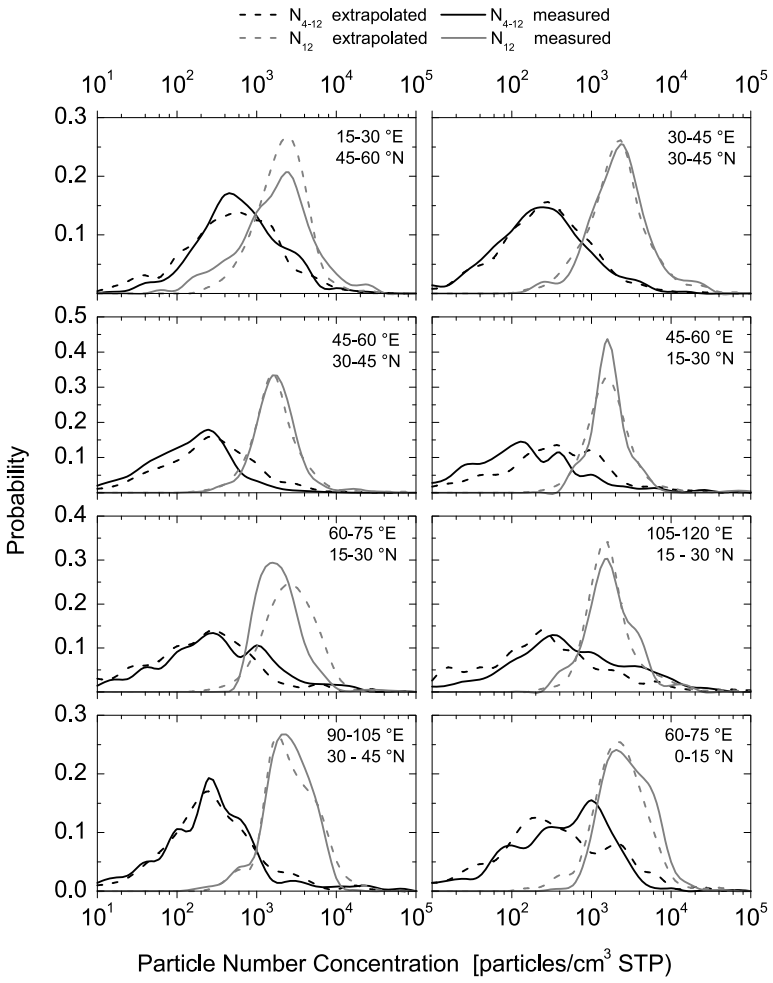

Fig. 4. Probability density functions for $N_{4–12}$, and N_{12}, for eight 15° × 15° geocells, once based on measured data only, and once based on trajectory-extrapolated data with at least 24 h time difference between measurement and extrapolation. Extrapolated data from the cell, in which the measurement occurred were also excluded. For this comparison, an aging parameter of $\tau = \infty$ was used.

trajectories that passed into the geocell but which originated from aircraft locations outside of the cell. Separately, for each geocell, we saved aerosol data if any forward or backward trajectory touched the respective geocell after a delay of at least 24 h between the time at the starting point of the trajectory and the time at which the trajectory touched the geocell. Data extrapolated from the cell, in which the measurement occurred were also excluded. Again, Probability Distribution Function (PDFs) were calculated with $\tau = \infty$ for these extrapolated data and compared to the PDFs of the direct measurements. Figure 4 shows the $N_{4–12}$ and N_{12} PDFs in eight geocells for the two cases measured data only and trajectory-extrapolated data only. The respective cells are the ones with the highest number of measurement data and thus with the best statistics. With a slight shift to lower concentrations, the results for N_{18} (not shown) are very similar to N_{12}. For N_{12}, seven out of eight geocells show a visually excellent agreement, only for the geocell 60–75°E and 15–30°N the extrapolated PDF maximum is ∼60% higher. For $N_{4–12}$, for six out of eight cells, the agreement is good, one geocell shows a clearly higher, one geocell a clearly lower PDF maximum. Interestingly, for all cases, the width of the two compared curves agrees well. This overall agreement is a first indication that extrapolating the particle measurements along UT/LMS trajectories within the given limits is valid.

3.2. External validation

In situ data collected by research aircraft in two atmospheric regions were compared to CARIBIC aerosol data. Except for two CARIBIC flights to Houston, Texas, none of the two regions had been touched by any CARIBIC flight (cf. Fig. 1, top panel). Thus, mostly trajectory-extrapolated data were compared to the external in situ measurements. The first external data set was discussed by Clarke and Kapustin (2002) in their review for the Pacific Ocean and is mainly based on data from the Pacific Exploratory Missions Tropics A/B (PEMT-A/B). For the comparison, we chose the geocell −166° to −88° longitude × −47° to 36° latitude, which contains 90% of their data. The PEMT-A/B data were corrected to STP conditions. As 85% of the CARIBIC in the comparison region stem from flight altitudes

between 27.000 and 39.000 feet, but only 50% of the available PEMT-A/B data, the use of the PEMT-A/B data was restricted to this altitude range. CARIBIC data were only used when they occurred during the four months (March, May, September and November), in which the PEMT-A/B flights took place. Altogether, about 4800 extrapolated data points (CARIBIC) were compared to about 7500 in situ measured data points (PEMT-A/B). The 'CN' channel of Clarke and Kapustin is directly comparable to the CARIBIC channel N_{12} whereas their channel 'UCN' is based on data from a TSI-3025 CPC, nominally counting particles above 3 nm diameter. Thus, we would expect the CARIBIC channel N_{4-12} to indicate systematically lower concentrations compared to the difference of UCN-CN. The small differences in the threshold diameters is acceptable considering other uncertainties like for instance associated with different inlet transmission efficiencies, which are estimated to be on the order of 20–30%.

The calculated PDFs are displayed in Fig. 5. The two Aitken mode PDFs, N_{12} and CN, show a similar width, only the maximum of CN is slightly lower than the N_{12} maximum. A much larger difference is found for the nucleation mode particles, the UCN-CN maximum is located at higher concentrations compared to the N_{4-12} maximum. For these particles, not only the PDF maximum but also width and shape of the PDFs are different. Instrumental reasons, that is, different inlet sampling efficiencies and different particle counters, cannot account for such clear differences [cf. Transport and Chemical Evolution over the Pacific (TRACE-P) comparison below]. Potential reasons might be different flight strategies (frequency of close-to- or in-cloud measurements) or the large temporal and spatial separation (relatively large PEMT-A/B area).

The second external data set stems from the TRACE-P experiment (Jacob et al., 2003). 90% of the available TRACE-P aerosol data were measured in the geocells limited by 125–149° in longitude and 26–35° in latitude. In this area, 93% of the data fall into the altitude range from 27.000 to 39.000 feet, close to the CARIBIC data (100%). The aerosol instrumentation of TRACE-P was similar to the payload used to derive the Clarke and Kapustin data, however, for TRACE-P, the authors give slightly different lower threshold diameters for the CPCs of 4 and 11 nm, respectively. Again, only CARIBIC data during the months of the TRACE-P experiment (February to April) were used. Altogether, about 2500 extrapolated data points (CARIBIC) were compared to about 760 in situ measured data points (TRACE-P). The PDFs of TRACE-P N_{11} and CARIBIC N_{12} in Fig. 6 agree very well in peak and width. Whereas the PDF of TRACE-P N_{4-11} is noisier, it still agrees well in peak and width with the CARIBIC N_{4-12} PDF. This good agreement in both particle size ranges obtained with similar instrumentation as in the PEMT-A/B experiments indicates that instrumental reasons are unlikely for the differences in the PEMT-A/B PDFs.

We emphasize that in both comparisons with aerosol data collected on research aircraft no aging of the extrapolated CARIBIC particle concentrations was used, that is, $\tau = \infty$. Any such particle aging did not improve the agreement of the respective PDFs. The same holds for all further results shown in this paper.

4. Results

4.1. Maps of UT/LMS particle number concentrations

With the 8 yr of combined CARIBIC data, global maps of aerosol statistics were constructed by sorting the data into geocells spanning 15° × 15° longitude × latitude. For statistical reasons, that is, insufficient data coverage at smaller scales, which might lead to grid cells with data from only one or two meteorological situations, a division into a finer grid or seasons, was not realized. Consequently, the shown concentration maps represent annual averages. Only data at pressures less than 500 hPa (above ~5.6 km altitude) were used for these maps, which mainly

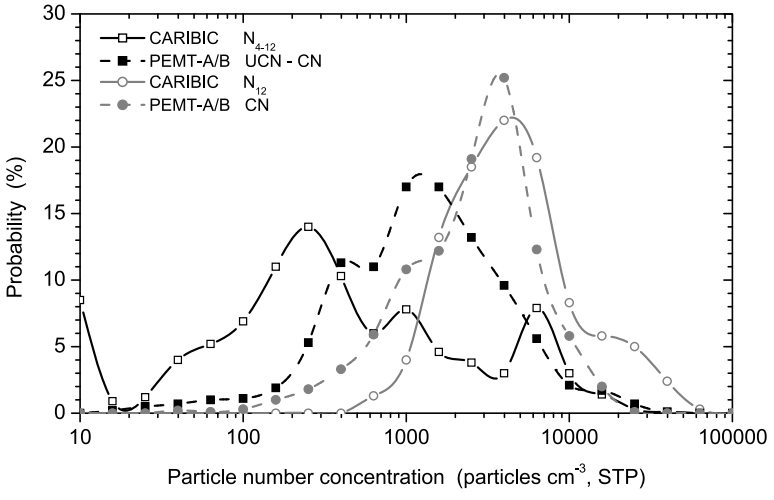

Fig. 5. Probability density functions of measured and extrapolated particle concentrations. Extrapolated data are from CARIBIC flight routes (N_{4-12}, N_{12}) transported via forward and backward trajectories to the comparison geocell of the PEMT-A/B data set (measured data, UCN-CN and CN). For this comparison, an aging parameter of $\tau = \infty$ was used.

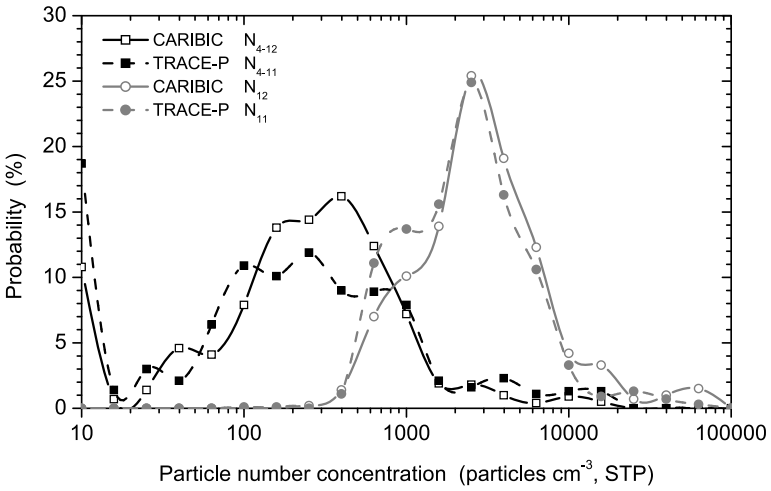

Fig. 6. Probability density functions of particle concentrations extrapolated from CARIBIC flight routes ($N_{4–12}$, N_{12}) via forward and backward trajectories to the comparison geocell of the TRACE-P experiment ($N_{4–11}$, N_{11}). For this comparison, an aging parameter of $\tau = \infty$ was used.

represent the UT/LMS region (cf. Fig. 1, bottom panel). At least 300 data points per geocell were required before results were reported in order to grant a minimum statistical significance for each cell.

The variability of the data was visualized by plotting maps of the percentiles 10th, 25th, 50th, 75th and 90th in Figs 7 and 8 for $N_{4–12}$ and N_{12}, respectively. Above a relatively even background at higher latitudes, four tropical/subtropical regions stand out in Fig. 7 in terms of $N_{4–12}$: Tropical Central and Western Africa with the adjacent Atlantic, South America, the Caribbean and Southeast Asia, where both lowest and highest concentrations were found. These regions of strong particle formation in the UT/LMS coincide with regions of frequent deep convective clouds, as shown by ISCCP data (http://isccp.giss.nasa.gov/products/browsed2.html) as well as satellite-based radar measurements (Liu and Zipser, 2005). Deep convection with both scavenging processes and strong vertical transport of particle precursors is the most likely cause of the resulting distributions of $N_{4–12}$ in the upper tropical troposphere (Weigelt et al., 2009). The influence of stratospheric air masses, which are more homogenous and are less frequently affected by deep convection, is indicated by the smaller variability of $N_{4–12}$ at high latitudes compared to low latitudes (cf. 10th and 9th percentiles and Fig. 1, top panel). Strong gradients (difference of three colour steps or more in adjacent cells) are partly caused by a dominance of tropospheric measurements in one cell and stratospheric measurements in the neighbouring cell, which is the case for instance over and west of South America.

Distribution and variability of N_{12} in Fig. 8 is at first glance similar to that of $N_{4–12}$. However, here the tropical regions of Africa, South America and Southeast Asia also stand out with the highest concentration levels at the 10th and the 90th percentile distributions. Relatively high concentrations of N_{12} at times were found over most of the mapped regions (90th percentile), which might be attributed to the longer lifetime of these particles compared to $N_{4–12}$ particles.

4.2. Zonal averages

By combining all data in latitudinal bands, meridional profiles of number concentrations were calculated for boreal summer (April–September) and winter (October–March) half years. Figure 9 gives these zonal results for $N_{4–12}$ and N_{12}. Additionally, for $N_{4–12}$, 75th percentiles are displayed in Fig. 9 to visualize the relatively rare events of high concentrations. Whereas the median of N_{12} shows a broad tropical maximum in summer, the meridional distribution of $N_{4–12}$ indicates strongest new particle formation in the northern hemispheric tropics and mid-latitudes. The tropical particle formation falls together with the average position of the Intertropical Convergence Zone (ITCZ) and hence deep convective cloud occurrence. The particle formation at northern mid-latitudes may have different reasons such as the increased availability of precursor gases (e.g. SO_2) over mid-latitude continents together with increasing solar radiation in boreal summer, leading to potentially higher concentrations of particle precursor gases. In winter, clear southern hemispheric maxima in N_{12} and $N_{4–12}$ are seen in accordance with the movement of the ITCZ. The respective particle concentrations are higher than the corresponding northern hemispheric summer values. A reason for this difference is not obvious, but of course the spatial measurement coverage in the Southern Hemisphere is much smaller than in the Northern Hemisphere (cf. Fig. 1, top panel). Hence, the magnitude of the southern hemispheric peaks, not the location, could be a statistical artefact. Northern mid-latitudes still exhibit somewhat elevated values of $N_{4–12}$ in winter.

4.3. Vertical profiles

Three different kinds of vertical profiles were analysed. First, all measured and extrapolated data together were sorted into pressure bins, separately for the tropics (−23°S to 23°N; Fig. 10, top panel) and the extratropics north of 23°N (Fig. 10, bottom

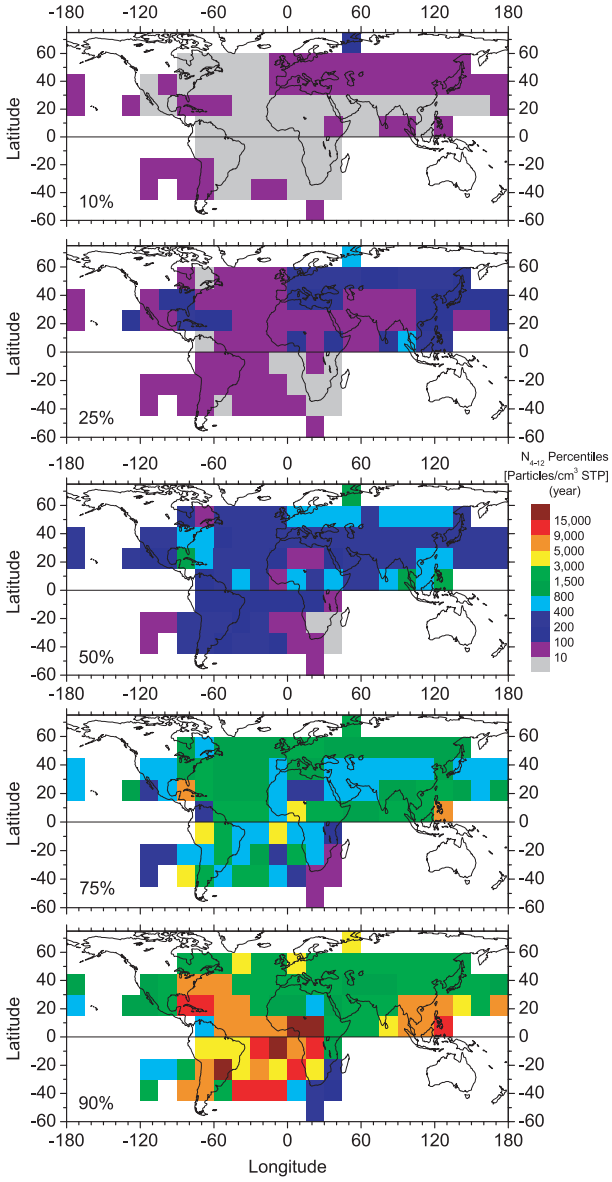

Fig. 7. Annual maps of measured and extrapolated number concentrations of particles between 4 and 12 nm diameter (N_{4-12}, particles cm^{-3} STP) in 15° × 15° geocells. Plotted are the 10th, 25th, 50th, 75th and 90th percentiles.

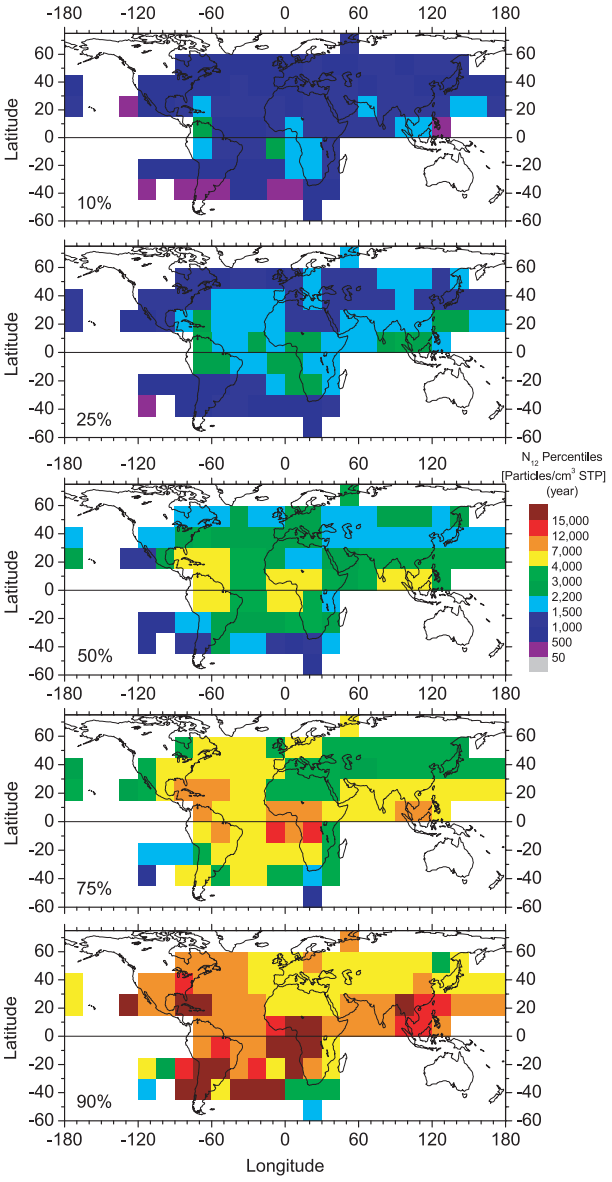

Fig. 8. Annual maps of measured and extrapolated number concentrations of particles ≥ 12 nm diameter (N_{12}, particles cm^{-3} STP) in 15° × 15° geocells. Plotted are the 10th, 25th, 50th, 75th and 90th percentiles.

panel). As the CARIBIC aircraft is based in Germany, the extratropical profile is dominated by data obtained during ascents from and descents towards Frankfurt, Germany. The tropical profile in Fig. 10a shows the frequently observed 'C-shape' for nucleation and Aitken mode particles with high concentrations near the surface, a minimum around 500 hPa followed by an increase towards the highest flight levels (de Reus et al., 2001; Schröder et al., 2002; Singh et al., 2002; Krejci et al., 2003). As well documented in the literature (e.g. Brock et al., 1995; Spracklen et al., 2005), the tropopause region exhibits favourable conditions for new particle formation. At altitudes corresponding to less than 800 hPa, the CARIBIC aircraft is near the airports, often in dense air traffic. The qualitative impression of both, lowest and highest N_{4-12} values occurring in the tropics is borne out by comparing the corresponding percentiles in Fig. 10 (top and bottom panels). The likely reason is the high frequency of tropical deep convective clouds, acting both as particle source but also as particles sink (Clarke et al., 1998; Weigelt et al., 2009). Lowest concentrations were found in the pressure interval 300 to 600 hPa. The concentration increase

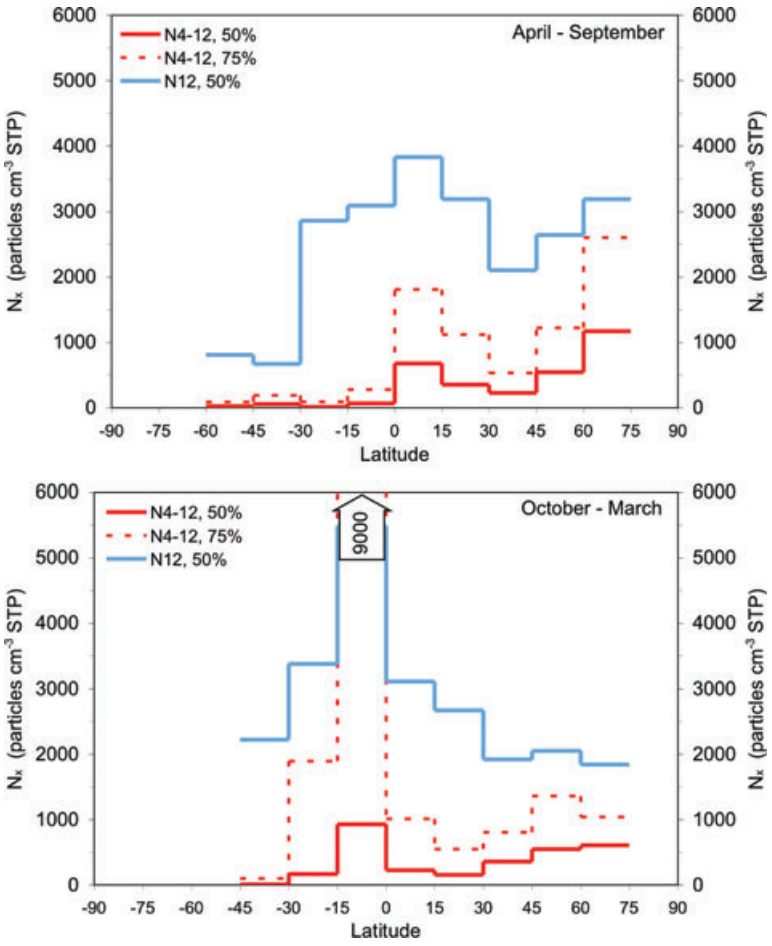

Fig. 9. Zonal median values of N_{12} and $N_{4–12}$ (particles cm^{-3} STP) in the upper troposphere and lower stratosphere in the boreal summer (April–September) and winter (October–March) half years. For the latter, 75th percentiles are plotted as well.

towards the stratosphere is larger in the tropics in both $N_{4–12}$ and N_{12}.

A second approach uses the concept of potential vorticity (PV; http://amsglossary.allenpress.com/glossary/search?id=potential-vorticity), which ranges from 0.3 to 0.5 PVU (1 PVU = 10^{-6} K m^2 kg^{-1} s^{-1}) in the lower and middle troposphere, and reaches 1 PVU in the upper troposphere. A strong increase in static stability leads to much higher values of PV in the stratosphere (Hoskins, 1991). With this discontinuity, a dynamic tropopause is defined at about 2 PVU. By using PV as vertical coordinate concentration profiles in the lowermost stratosphere were generated, with PV values ranging from 0 to 15 PVU. In Fig. 11, PV-classified profiles are shown in terms of 25th, 50th and 75th percentiles for both, $N_{4–12}$, and N_{12}. To increase statistical relevance, only PV bins with at least 500 data points are displayed. The profiles for boreal winter (uppermost graph) show for most percentiles a 'monotonic decrease from the tropopause around PV = 2 PVU (Hoskins, 1991) towards higher PV values deeper into the stratosphere. This feature is in agreement with prevailing downward transport from the lower stratosphere and hence the measurement of aged air masses with reduced particle number concentrations. In spring, there seems to be a first indication for a particle concentration maximum at the upper border of the mixing layer between the troposphere and the lowermost stratosphere, the extratropical tropopause transition layer (ExTL, e.g. WMO, 2002; Zahn and Brenninkmeijer, 2003; Pan et al., 2004; Hegglin et al., 2009). These maxima in $N_{4–12}$ as well as N_{12} above 6 PVU are even more pronounced in summer. In autumn, N_{12} decreases almost monotonically with increasing PV, as in winter, but $N_{4–12}$ shows an indifferent behaviour, somehow similar to spring. Due to the flight altitude of the CARIBIC aircraft (8–12 km, cf. Fig. 1, bottom panel) air masses from the upper border of the ExTL (i.e. with high PV values) are only probed when the local tropopause is low. For CARIBIC, this is mainly the case when measuring in tropopause folds in the vicinity of the jet stream (cf. www.knmi.nl/samenw/campaign_support/CARIBIC). Hence, the measurements at high PV are biased towards this specific meteorological situation. In tropopause folds, mixing of stratospheric and tropospheric air can lead to new particle formation (Zahn et al., 2000; Young et al., 2007). Hence, it is not clear if particle formation takes place at the upper border of

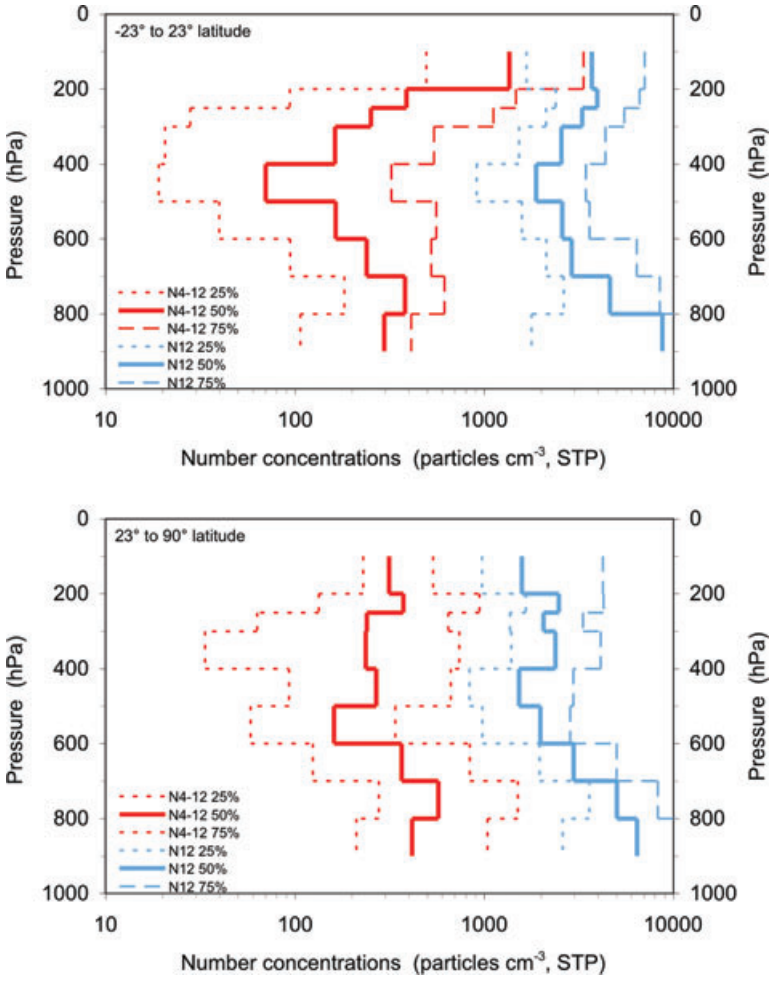

Fig. 10. Top panel: Pressure-dependent percentiles 25th, 50th and 75th of $N_{4–12}$ and N_{12} (particles cm^{-3} STP) for the region –23–23° latitude (tropics). Bottom panel: Pressure-dependent percentiles 25th, 50th and 75th of $N_{4–12}$ and N_{12} (particles cm^{-3} STP) north of 23° latitude (subtropics and mid-latitudes).

the ExTL and these particles are transported downwards to flight altitudes or, more likely, particle formation is cause by mixing of stratospheric and tropospheric air masses in connection with tropopause folds. Only some 0.2% of all measured data extended beyond 60°N. Thus, chances of the vertical profiles being influenced by processes connected to the Arctic polar vortex (e.g. Borrmann et al., 1993) are rather small.

Third, vertical profiles of the ratios of N_{12} to CO and O_3, respectively, were generated and are displayed as function of PV in Fig. 12. As CO is a typical tracer for boundary layer air and O_3 for stratospheric air, these ratios might reveal information on the origin of the particles. The vertical N_{12}/O_3 profiles show a strong decrease with increasing PV in all seasons. The shapes of the curves are very similar over the year with some variation in absolute values, caused by the subsidence of stratospheric air in winter/spring and the injection of tropospheric air into the LMS in summer/autumn. In the troposphere, mostly N_{12} values are high and O_3 values are low. In contrast, in the stratosphere O_3 is increasing with altitude/PV, whereas N_{12} values are decreasing in the first few kilometres above the tropopause. Consequently in the ExTL, a negative correlation is found.

Different to N_{12}/O_3, the N_{12}/CO ratio vertical profile shows a strong seasonal variation. In boreal winter and at first approximation also in autumn, N_{12}/CO stays almost constant with PV/altitude above the tropopause (PV $\approx$ 2 PVU). In spring and summer, there is, however, a strong and clear increase towards higher PV values. These curve shapes might be partly explained by the relatively high particle number concentrations at high PV values for the two seasons (cf. Fig. 11) as well as the general decrease in CO with increasing PV/altitude above the tropopause. Moreover, there is a large variability in the N_{12}/CO ratio, particularly in spring and summer, much larger than the variability in CO alone within the respective seasons. Hence, this variability is rather controlled by particle concentrations (cf. Fig. 11). According to the variability-lifetime hypothesis (Junge, 1974) this indicates a much shorter lifetime for N_{12} compared to CO, the latter being about six weeks in summer and a few months in winter in the UT. As the particle lifetime is relatively short, observed concentrations are likely dominated by local processes and not

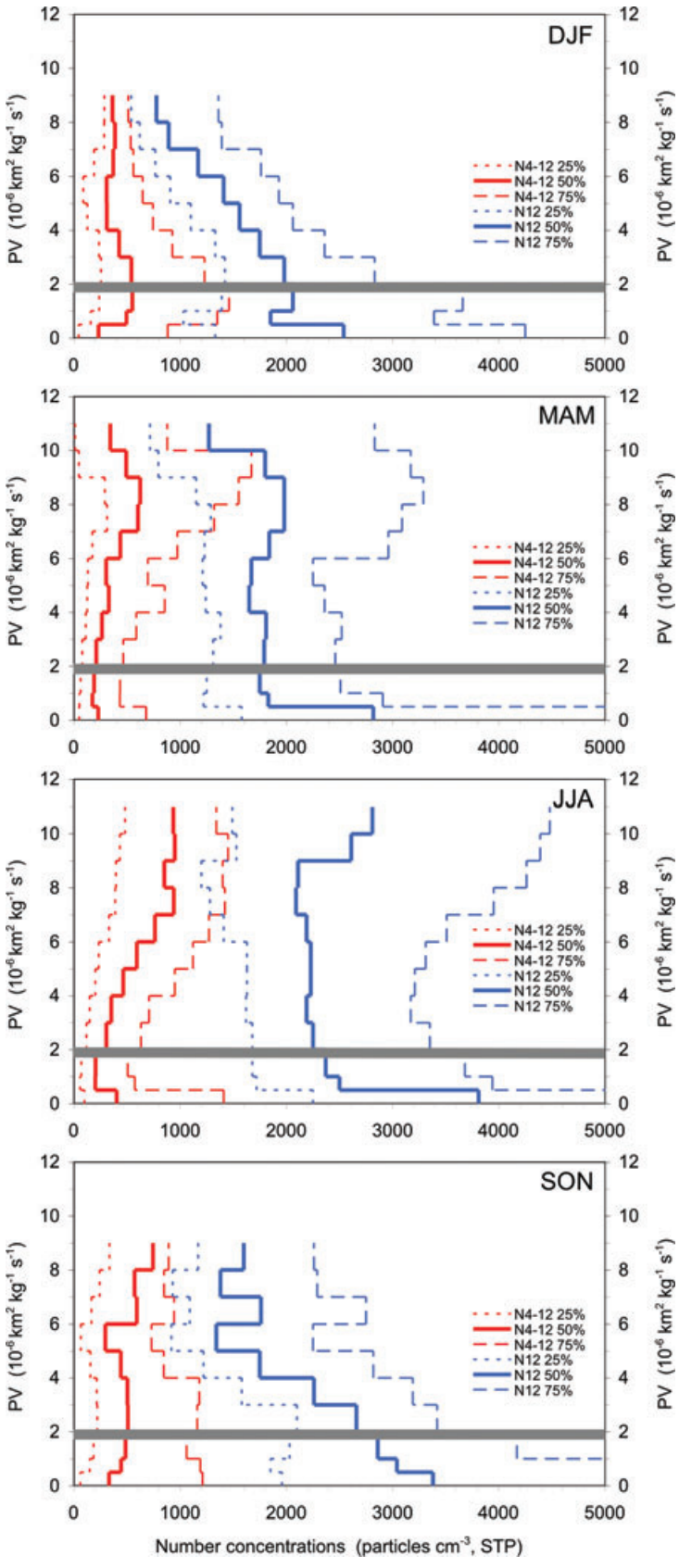

Fig. 11. Percentiles 25th, 50th and 75th of N_{4-12} and N_{12} (particles cm^{-3} STP) classified by potential vorticity (PV).

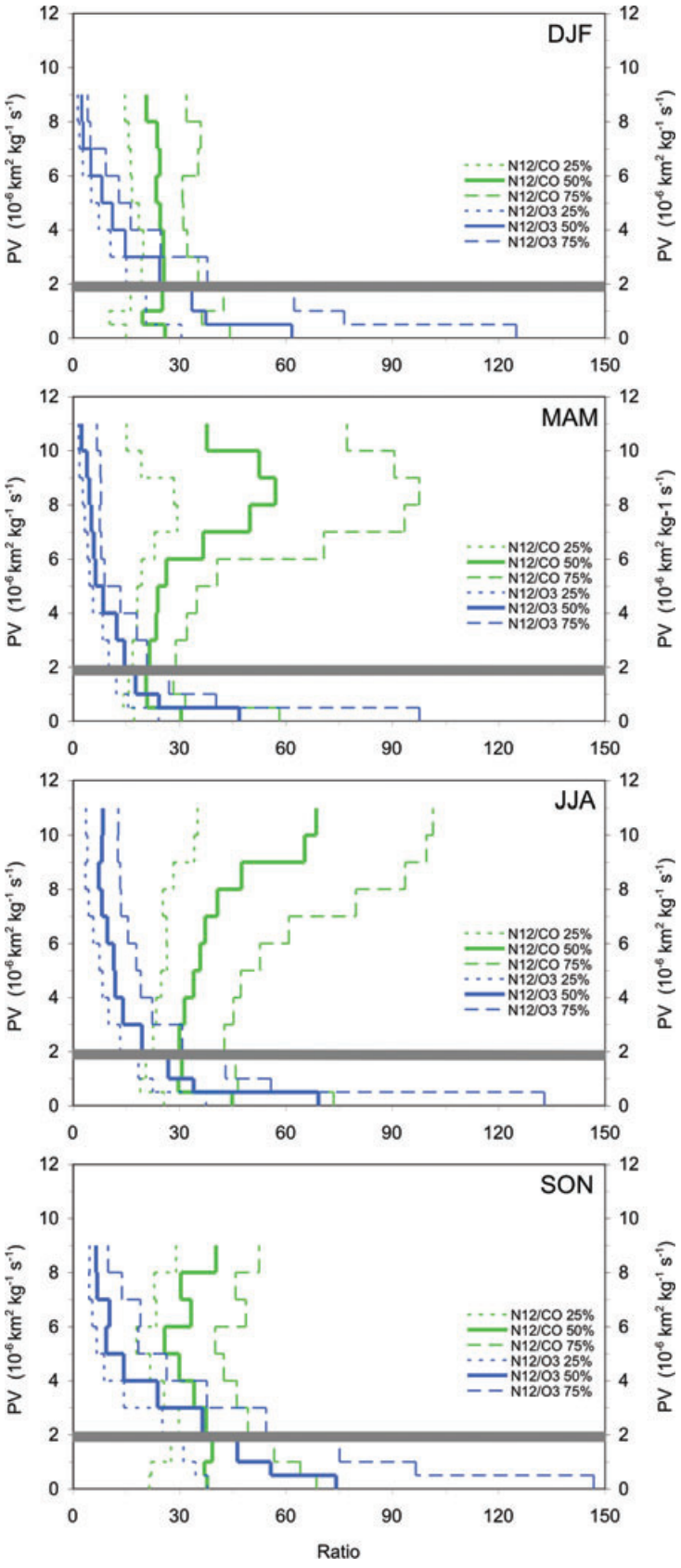

Fig. 12. Percentiles 25th, 50th and 75th of N_{12}/CO (green) and N_{12}/O_3 (blue) (in (particles cm^{-3} STP)/ ppb) classified by potential vorticity (PV).

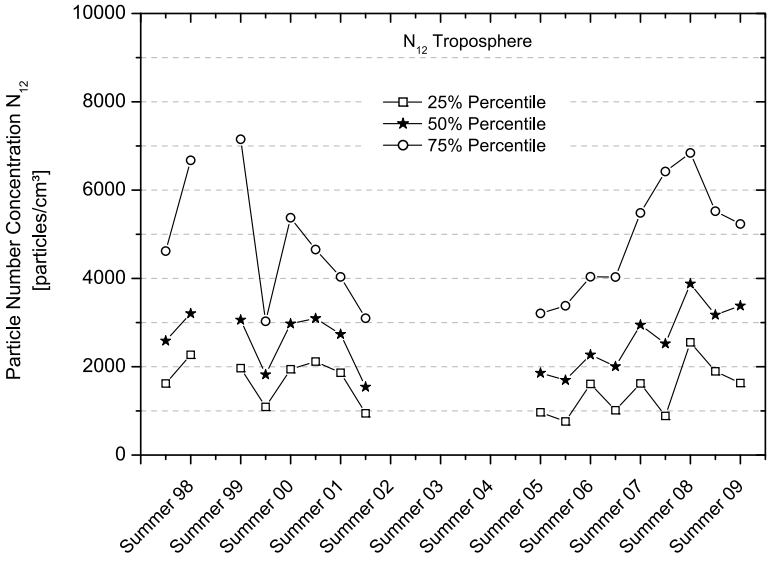

Fig. 13. Seasonal 25th, 50th and 75th percentiles for Aitken mode particles (N_{12}) in the upper troposphere over Europe.

by slower long-range transport, for example, from the tropics (e.g. Hoor et al., 2004). Again, the mixing of tropospheric and stratospheric air masses is probably the most dominant of local processes.

4.4. Long-term trend

The long duration of the CARIBIC project suggests a search for long-term trends in the measured aerosol properties. For this purpose, we extended the data set beyond the time period covered by cloud information till the end of 2009, thus adding another 52 flights. During the course of the project, the routes changed substantially. However, all routes started in Germany. To homogenize the data and to exclude effects due to different flight routes, we restricted the data set for the trend analysis to the geographical region of longitudes -10° to 35° and latitudes 37° to 55°, roughly corresponding to Europe without its northern part. The remaining set of measured particle concentrations is divided into two subpopulations, one, covering all 77 flights with LTU (1997–2002), and the other, with 123 LH flights (2004–2009). As the concentration of the nucleation mode particles, because of their short lifetime, is probably more affected by the flight statistics (day/night), we discuss here only the Aitken mode particles, N_{12}. In Fig. 13, the seasonal 25th, 50th and 75th percentile concentrations for the upper troposphere and the whole CARIBIC period are displayed. Only seasons with at least four flights were considered. In a second representation, arithmetic means and the percentiles 10th, 50th and 90th for these two subpopulations are shown in Table 1. These statistics were calculated separately for tropospheric, stratospheric and for the combined data.

The graphical representation (Fig. 13) first suggests a weak decrease of N_{12} in the first period and a stronger increase in the second period. However, the season-to-season or year-to-year variability is even larger than the 'trend', at least for the first

Table 1. Number of measurements (n), arithmetic means (m) and 10th, 50th and 90th percentiles of N_{12} (particles cm^{-3} STP) over Europe for two CARIBIC subpopulations: one, covering all 77 flights with LTU (1997–2002), the other with 123 Lufthansa (LH) flights (2004–2009)

	N_{12}				
Year	n	m	0.1	0.5	0.9
LTU_all	235 833	3883	882	2306	7260
LH_all	388 506	3928	738	2498	7674
d%_all	–	1	−16	8	6
LTU_trop.	146 028	4201	934	2492	7846
LH_trop.	182 592	4787	743	2729	10 048
d%_trop.	–	14	−20	10	28
LTU_strat.	89 805	3366	774	2104	6238
LH_strat.	205 914	3166	735	2319	5938
d%_strat	–	−6	−5	10	−5

Note: all, all data; trop., tropospheric data only; strat., stratospheric data only; d%, the relative change from the LTU to the LH period, expressed as percentage of the LTU value.

period. Hence, for the whole data set, a clear statement about a trend cannot be made; only the increase within the second period is considerable. Comparing the two subpopulations as a whole (Table 1), the N_{12} median shows a ∼10% increase for all three spatial regimes. In order to test if both data sets stem from the same basic population the 'Mann–Whitney U-test' (Pruscha, 2006) was applied. The results indicate a significant difference for each of the two subsets. There are two possible explanations for the observed 'trend' and the statistical difference between the two data sets. First, there is a real trend/increase in the submicrometre UT/LMS aerosol of the Northern Hemisphere in recent years. This trend could be caused by several reasons, for

example, changes in large-scale dynamics, changes in particle surface area (precursor gas and particle sink) or increasing SO_2 emissions over China (Smith et al., 2011) similar to the trend observed for the stratospheric aerosol (Hofmann et al., 2009). However, because of the aircraft changeover and hence two different aerosol inlets, sampling lines and slightly different flight altitudes (cf. Fig. 1, bottom panel), small differences in the two data sets are likely. The effects of the different aerosol inlets and sampling lines, although largely accounted for, by applying respective empirical corrections for particles losses, might explain the small differences in N_{12} between the two subpopulations, but not the increase within the LH data set alone. Hopefully, with the upcoming years of further CARIBIC measurements onboard the LH aircraft, the answer to the question of a trend will become clearer.

5. Conclusions

During the course of more than 11 yr, the intercontinental flights of the CARIBIC project covered substantial fractions of the northern hemispheric UT/LMS. When classified in $15^\circ \times 15^\circ$ geocells there are significant measured CARIBIC aerosol data in ca. 14% of all cells. The large-scale dynamics of the UT/LMS suggests extrapolating the measured aerosol data along backward and forward trajectories. Limiting these extrapolations to plus/minus two days about the respective measurements or to the last/next cloud contact, whatever occurs first, increased the data coverage to ca. 36% of the globe. Geostatistics of this rich data set identified four tropical/subtropical regions with enhanced particle concentrations above a relatively even background at higher latitudes: Tropical Central and Western Africa with the adjacent Atlantic, South America, the Caribbean and Southeast Asia. In these areas, both lowest and highest number concentrations occurred. Deep convection with both, scavenging processes and strong vertical transport of particle precursors is the most likely candidate process causing this finding. Combining all longitudes in meridional profiles confirmed the broad tropical concentration maximum, coinciding with the ITCZ, in particular in summer. At the same time, this combination yielded a secondary concentration maximum in mid-latitude summers, which we attribute mainly to the increased availability of precursor gases at mid-latitudes in connection with vertical transport or particle formation in connection with stratospheric air masses.

Sorting the data in the vertical elucidates the source regions further. Again, the tropics stand out with a concentration increase with height above the 500 hPa level, both for $N_{4–12}$ and N_{12}. With the potential vorticity as sorting parameter for the LMS, the seasonal groups March–April–May and June–July–August show concentration increases from the tropopause up likely indicating new particle formation in connection with tropopause folds.

In principle, one would expect that aerosol aging processes affect the measured number concentrations when following the trajectories backward or forward in time. Under the simple assumption of no particle source processes taking place within the plus/minus 2 d of analysis, coagulation should decrease number concentrations with time, in particular $N_{4–12}$. However, neither of the two comparisons with data from research campaigns nor a self-validation by comparing our aerosol measurements in given geocells with CARIBIC data extrapolated along trajectories into respective cells could be improved by allowing exponential concentration decays with time constants shorter than the trajectory lengths (48 h). This is an unexpected result, because depending on the given particle sizes and concentrations, a decrease of about 5–30% in number concentration within 2 d due to coagulation can be estimated (monodisperse aerosol, Baron and Willeke, 2001). Even when considering that the ambient particle size range of particles measured in the CPC size window 4–12 nm is rather 6–20 nm because the particles partially evaporate in the inlet sampling line (Hermann et al., 2001) at least for the $N_{4–12}$ particles, an effect should be visible because of their short particle lifetime (cf. Williams et al., 2002, table 2). Our findings may suggest a slower aerosol aging in a cloud-free UT/LMS or that the assumptions underlying our simple decay approach are not valid. The latter might be the case if there is a kind of dynamic equilibrium, that is, particle formation starting at different times after a cloud contact would compensate the reduction in particle number due to coagulation, which was already observed by Weigelt et al. (2009).

Finally, the extent of the CARIBIC data set suggested a search for long-term trends. As all flights started from and returned to a base in Germany, we restricted the trend search to a geocell roughly encompassing Europe. Because of the aircraft changeover between 2002 and 2004, we compared the Aitken mode (N_{12}) subpopulations 1997–2002 and 2004–2009. The difference between the two periods is small (+10%) and no clear trend is seen. A significance test (Mann–Whitney U-test) indicated, however, this difference to be statistically significant for all confidence intervals between 80 and 95%. More clearly, there is an increase in N_{12} within the second period from 2004–2009. Hence, there might be a positive trend, that is, an increase in the submicrometre UT/LMS particle number concentration in recent years.

CARIBIC flights continue at a rate of roughly four long-distance flights per month, extending the CARIBIC database in the UT/LMS both, in terms of geographic coverage, and long-term trends in atmospheric composition.

6. Acknowledgments

The authors are deeply grateful to Lufthansa Passage Airlines and Lufthansa Technik (in particular, Andreas Waibel, Thomas Dauer, Detlev Hartwig, Sven Dankert and Jörg Rohwer) for their support of CARIBIC and to Dieter Scharffe and Claus Koeppel (Max Planck Institute for Chemistry) for the equipment support and container operation. The development of the CARIBIC system was financially supported by the German Ministry of

Education and Science (AFO 2000 program) and its operation benefited and benefits from the European Commission's DGXII Environment RTD 4th, 5th, 6th and 7th Framework programs.

References

Baron, P. A. and Willeke, K. 2001. Gas and particle motion. In: *Aerosol Measurement—Principles, Techniques, and Applications* (eds P. A. Baron and K. Willeke). John Wiley & Sons, New York, NY, 61–82.

Borrmann, S., Dye, J. E., Baumgardner, D., Wilson, J. C., Jonsson, H. H. and co-authors. 1993. In-situ measurements of change in stratospheric aerosol and the N_2O-aerosol relationship inside and outside of the polar vortex. *Geophys. Res. Lett.* **20**, 2559–2562.

Brenninkmeijer, C. A. M., Crutzen, P. J., Fischer, H., Güsten, H., Hans, W. and co-authors. 1999. CARIBIC—civil aircraft for global measurements of trace gases and aerosols in the tropopause region. *J. Atmos. Ocean. Technol.* **16**, 1373–1383.

Brenninkmeijer, C. A. M., Crutzen, P., Boumard, F., Dauer, T., Dix, B. and co-authors. 2007. Civil aircraft for the regular investigation of the atmosphere based on an instrumented container: the new CARIBIC system. *Atmos. Chem. Phys.* **7**, 4953–4976.

Brock, C. A., Hamill, P., Wilson, J. C., Jonsson, H. H. and Chan, K. R. 1995. Particle formation in the upper tropical troposphere: a source of nuclei for the stratospheric aerosol. *Science* **270**, 1650–1653.

Clarke, A. D. and Kapustin, V. N. 2002. A pacific aerosol survey. Part I: A decade of data on particle production, transport, evolution, and mixing in the troposphere. *J. Atmos. Sci.* **59**, 363–382.

Clarke, A. D., Varner, J. L., Eisele, F., Mauldin, R. L. and Tanner, D. 1998. Particle production in the remote marine atmosphere: cloud outflow and subsidence during ACE 1. *J. Geophys. Res.* **103**, 16397–16409.

Hegglin, M. I., Boone, C. D., Manney, G. L. and Walker, K. A. 2009. A global view of the extratropical tropopause transition layer from Atmospheric Chemistry Experiment Fourier Transform Spectrometer O_3, H_2O, and CO. *J. Geophys. Res.* **114**, D00B11, doi:10.1029/2008JD009984.

Heintzenberg, J., Hermann, M., Martinsson, B. G. and Papaspiropoulos, G. 2002. Number and sulfur derived 3-parameter aerosol size distributions in the tropopause region from CARIBIC flights between Germany and the Indic. *J. Aerosol Sci.* **33**, 595–608.

Hermann, M., Brenninkmeijer, C. A. M., Slemr, F., Heintzenberg, J., Martinsson, B. G., Schlager, H., van Velthoven, P. J., Wiedensohler, A., Zahn, A. and Ziereis, H. 2008. Submicrometer aerosol particle distributions in the upper troposphere over the mid-latitude North Atlantic – Results from the third route of "CARIBIC". *Tellus* **60B**, 106–117.

Hermann, M. and Wiedensohler, A. 2001. Counting efficiency of condensation particle counters at low-pressures with illustrative data from the upper troposphere. *J. Aerosol Sci.* **32**, 975–991.

Hermann, M., Stratmann, F., Wilck, M. and Wiedensohler, A. 2001. Sampling characteristics of an aircraft-borne aerosol inlet system. *J. Atmos. Ocean. Technol.* **18**, 7–19.

Hermann, M., Heintzenberg, J., Wiedensohler, A., Zahn, A., Heinrich, G. and co-authors. 2003. Meridional distributions of aerosol particle number concentrations in the upper troposphere and lower stratosphere obtained by Civil Aircraft for Regular Investigation of the Atmosphere Based on an Instrument Container (CARIBIC) flights. *J. Geophys. Res.* **108**, doi:10.1029/2001JD0010077.

Hermann, M., Adler, S., Caldow, R., Stratmann, F. and Wiedensohler, A. 2005. Pressure-dependent efficiency of a condensation particle counter operated with FC-43 as working fluid. *J. Aerosol Sci.* **36**, 1322–1337.

Hermann, M., Wehner, B., Bischof, O., Han, H.-S., Krinke, T. and co-authors. 2007. Particle counting efficiencies of new TSI condensation particle counters. *J. Aerosol Sci.* **38**, doi: 10.1016/j.jaerosci.2007.1005.1001.

Hofmann, D., Barnes, J., O'Neill, M., Trudeau, M. and Neely, R. 2009. Increase in background stratospheric aerosol observed with lidar at Mauna Loa Observatory and Boulder, Colorado. *Geophys. Res. Lett.* **36**, L15808, doi:15810.11029/12009GL039008.

Hoor, P., Gurk, C., Brunner, D., Hegglin, M. I., Wernli, H. and Fischer, H. 2004. Seasonality and extent of extratropical TST derived from in-situ CO measurements during SPURT. *Atmos. Chem. Phys.* **4**, 1427–1442.

Hoskins, B. J. 1991. Towards a PV-theta view of the general circulation. *Tellus* **43A**, 27–35.

Jacob, D. J., Crawford, J. H., Kleb, M. M., Connors, V. S., Bendura, R. J. and co-authors. 2003. Transport and Chemical Evolotion over the Pacific (TRACE-P) aircraft mission: design, execution, and first results. *J. Geophys. Res.* **108**, doi:10.1029/2002JD003276.

Jaenicke, R. 1978. On the dynamics of atmospheric Aitken particles. *Berichte Bunsengesellschaft Phys.* **82**, 1198–1202.

Jaenicke, R. 1988. Aerosol physics and chemistry. In: *Numerical Data and Functional Relationships in Science and Technology* (ed. G. Fischer). Springer-Verlag, Heidelberg, 391–457.

Junge, C. E. 1974. Residence time and variability of tropospheric trace gases. *Tellus* **26**, 477–488.

Krejci, R., Ström, J., de Reus, M., Hoor, P., Williams, J. and co-authors. 2003. Evolution of aerosol properties over the rain forest in Surinam, South America, observed from aircraft during the LBA-CLAIRE 98 experiment. *J. Geophys. Res.* **108**, 4561, doi:4510.1029/2001JD001375.

Liu, C. and Zipser, E. J. 2005. Global distribution of convection penetrating the tropical tropopause. *J. Geophys. Res.* **110**, D23104, doi:23110.21029/22005JD006063.

Pan, L. L., Randel, W. J., Gary, B. L., Mahoney, M. J. and Hintsa, E. J. 2004. Definitions and sharpness of the extratropical tropopause: a trace gas perspective. *J. Geophys. Res.* **109**, D23103, doi:23110.21029/22004JD004982.

Pruscha, H. 2006. Statistical Method Book: Algorithms, Case Studies, Program Codes. Springer, Berlin, Germany, 412pp.

de Reus, M., Krejci, R., Williams, J., Fischer, H., Scheele, R. and co-authors. 2001. Vertical and horizontal distributions of the aerosol number concentration and size distribution over the northern Indian Ocean. *J. Geophys. Res.* **106**, 28629–28641.

Rossow, W. B. and Schiffer, R. A. 1991. ISCCP cloud data products. *Bull. Am. Meteorol. Soc.* **72**, 2–20.

Scheele, M. P., Siegmund, P. C. and van Velthoven, P. F. J. 1996. Sensitivity of trajectories to data resolution and its dependence on the starting point: in or outside a tropopause fold. *Meteorol. Appl.* **3**, 267–273.

Schröder, F., Kärcher, B., Fiebig, M. and Petzold, A. 2002. Aerosol states in the free troposphere at northern midlatitudes. *J. Geophys. Res.* **107**, LAC 8-1–LAC 8-8.

Singh, H. B., Anderson, B. E., Avery, M. A., Viezee, W., Chen, Y. and co-authors. 2002. Global distribution and sources of volatile and nonvolatile aerosol in the remote troposphere. *J. Geophys. Res.* **107**, doi:10.1029/2001JD000486.

Smith, S. J., van Aardenne, J., Klimont, Z., Andres, R. J., Volke, A. and co-authors. 2011. Anthropogenic sulfur dioxide emissions: 1850–2005. *Atmos. Chem. Phys.* **11**, 1101–1116.

Spracklen, D. V., Pringle, K. J., Carslaw, K. S., Chipperfield, M. P. and Mann, G. W. 2005. A global off-line model of size-resolved aerosol microphysics: I. Model development and prediction of aerosol properties. *Atmos. Chem. Phys.* **5**, 2227–2252.

Stohl, A., James, P., Forster, C., Spichtinger, N., Marenco, A. and co-authors. 2001. An extension of Measurement of Ozone and Water Vapour by Airbus In-service Aircraft (MOZAIC) ozone climatologies using trajectory statistics. *J. Geophys. Res.* **106**, 7,757–727,776.

Weigelt, A., Hermann, M., van Velthoven, P. F. J., Brenninkmeijer, C. A. M., Schlaf, G. and co-authors 2009. Influence of clouds on aerosol particle number concentrations in the upper troposphere. *J. Geophys. Res.* **114**, D01204, doi:01210.01029/02008JD009805.

Williams, J., de Reus, M., Krejci, R., Fischer, H. and Strom, J. 2002. Application of the variability-size relationship to atmospheric aerosol studies: estimating aerosol lifetimes and ages. *Atmos. Chem. Phys.* **2**, 133–145.

WMO. 2002. Scientific assessment of ozone depletion: 2002. WMO Global Ozone Research and Monitoring Project Report 47. World Meteorological Organization, Geneva, Switzerland, 498pp.

Young, L.-H., Benson, D. R., Montanaro, W. M., Lee, S.-H., Pan, L. L. and co-authors. 2007. Enhanced new particle formation observed in the northern midlatitude tropopause region. *J. Geophys. Res.* **112**, D10218, doi:10210.11029/12006JD008109.

Zahn, A. and Brenninkmeijer, C. A. M. 2003. New directions: a chemical tropopause defined. *Atmos. Environ.* **37**, 439–440.

Zahn, A., Brenninkmeijer, C. A. M., Maiss, M., Scharffe, D., Crutzen, P. J. and co-authors. 2000. Identification of extratropical 2-way troposphere-stratosphere mixing based on CARIBIC measurements of O_3, CO, and ultrafine particles. *J. Geophys. Res.* **105**, 1527–1535.